Int. J. Heat Mass Transfer. Vol. 23, pp. 1003 1013
Pergamon Press Ltd. 1980. Printed in Great Britain

STUDY ON A HEAT PIPE

SHINZO SHIBAYAMA
Waseda University, Shinjuku-ku, Tokyo, Japan
and
SHINICHI MOROOKA
Nuclear Engineering Laboratory, Toshiba Corp.,
Kanagawa-ken, Japan

(*Received* 24 *February* 1979)

Abstract—The objective of this study was to obtain an understanding of heat pipe operating limits. Sintered powders were used as the wick, and pure water and Freon 113 as the working fluid. In this study, two types of experiments were undertaken. The first involved independent studies of wick characteristics, friction losses and capillary properties. The second involved the measurement of maximum heat transfer rates. The simplified model was developed for predicting the maximum heat transfer rates of capillary limits. The agreement between predicted and experimental maximum heat-transfer rates was excellent.

NOMENCLATURE

A_t, tube cross section [m^2];
A_w, wick cross section [m^2];
D_C, minimum pore diameter [m];
D_H, hydraulic diameter [m];
D_{in}, pipe inner diameter [m];
D_P, particle diameter [m];
D^*, diameter at thermocouple position [m];
f_K, friction factor;
H_I, H_F,
H_R, level [m];
h, equilibrium capillary height [m];
K_P, permeability [m^2];
L, latent vaporization heat [$J\,kg^{-1}$];
l, length [m];
l_p, heat pipe length [m];
m, mass flux [$Kg\,s^{-1}$];
N_{Re}, Reynolds number;
ΔP_l, viscous liquid pressure drop in a wick [$N\,m^{-2}$];
ΔP_C, maximum capillary pressure [$N\,m^{-2}$];
ΔP_V, viscous vapor pressure drop [$N\,m^{-2}$];
ΔP_g, gravitational head [$N\,m^{-2}$];
Q, volume flow rate [$m^3\,s^{-1}$];
Q_e, heat transfer rate [W];
q, heat flux [$W\,m^{-2}$];
T, temperature [°C];
T_V, vapor temperature [°C];
T_W, temperature of the inner wall [°C];
t, time [s];
u_f, velocity [$m\,s^{-1}$];
x, axial coordinate [m].

Greek symbols

Δ, difference symbol;
θ, contact angle [rad];
ν, kinematic viscosity [$m^2\,s^{-1}$];
ρ, density [$kg\,m^{-3}$];
σ, surface tension [$N\,m^{-1}$];
ϕ, inclination angle [rad];
ε, porosity;
λ_s, container thermal conductivity [$W\,m^{-1}\,°C$].

Subscripts

a, adiabatic;
c, condenser;
e, evaporator;
l, liquid;
max, maximum;
meas, measurement;
R, Freon 113;
w, water.

1. INTRODUCTION

THE HEAT pipe is a heat transfer device which can transport heat at high rates with a very small temperature gradient. The phenomena of evaporation, condensation and surface tension pumping of a liquid in a capillary wick are used to transfer latent vaporization heat continuously from one region to another. Main heat transfer performance limits of a low temperature heat pipe are boiling limits at which vapor bubbles formed by boiling may interrupt the flow of liquid into the evaporator wick and consequently limit the radial heat flux, and the wicking limits which have resulted from the inability of the capillary force of a wick to supply sufficient liquid to the evaporator.

The theoretical treatment concerning the performance limits of a heat pipe was first published by Cotter [1]. He concluded that the maximum heat-transfer rate that a heat pipe could support would depend on the ability of the capillary force to deliver liquid at a sufficient rate to maintain the equilibrium in the evaporator.

Phillips [2] and Kunz *et al.* [3] conducted an experimental study on wick capillary force, liquid flow

losses in a wick and critical heat flux, and conducted a qualitative investigation of the experimental results. On the other hand, studies using sintered powders or small particles as the wick were conducted by Ferrell and Johnson [4], Cosgrove [5] and Alexander [6], who used a simplified model of a heat pipe. However, no obvious result has been obtained due to a narrow range of experimental conditions and a use of a model heat pipe. Therefore, the authors tried to conduct an experimental study over a wider range of conditions, using an actual heat pipe (not a model heat pipe), and to develop a mathematical model to predict the maximum heat transfer rate. The capillary forces and pressure drop through the wick were measured independently of the heat pipe test.

2. DESCRIPTIONS OF WICKS STUDIED

Descriptions of wicks and fluid properties at room temperature used to measure the wick properties are given in Tables 1 and 2, respectively.

3. PRESSURE DROP THROUGH THE WICK

3.1. *Experiment outline*

Pressure drop though the wick was measured using a steady state method and an unsteady state method [5]. Drawings of the apparatus used are shown in Figs. 1 and 2, respectively. In a steady state method, pressure drop was measured by a manometer, while the flow-rates of air and other fluid was measured by an orifice and a flowmeter, respectively. In an unsteady state method, the time required for the water level in the tube above the sample to fall from H_I to H_F was measured.

Cosgrove [5] applied Darcy's Law [7] to this situation and calculated the permeability from the following equation,

$$K_P = \frac{A_t v_l l}{A_w g t} \ln \frac{H_I - H_R}{H_F - H_R} \tag{1}$$

where [7]

$$K_P = \frac{v_l \rho_l l Q}{A_w \Delta P_l} \left[\frac{\mathrm{d}P_l}{\mathrm{d}x} = \frac{v_l \dot{m}_l}{K_p A_w} \right]. \tag{2}$$

Table 1. Descriptions of wicks

	Material	Particle size range (μ)	Average particle size (μ)	Porosity
*J*1	Bronze	61 ~ 147	104	0.558
*J*2	Bronze	—	147	0.491
*J*3	Bronze	147 ~ 208	178	0.304
*J*4	Bronze	246	246	0.365
*J*5	Bronze	74 ~ 147	111	0.388
*J*6	Bronze	246 ~ 495	353	0.420
*J*7	Bronze	710 ~ 840	811	0.530
*J*8	Bronze	147 ~ 246	197	0.362
*J*9	Bronze	147 ~ 246	197	0.389
*J*10	Bronze	147 ~ 246	197	0.458
*J*11	Bronze	147 ~ 246	197	0.448
*J*12	Bronze	147 ~ 246	197	0.492
*J*13	Bronze	—	757	0.542
*J*14	Bronze	351 ~ 495	423	0.369
*J*15	Bronze	351 ~ 495	423	0.407
*J*16	Bronze	351 ~ 495	423	0.395
*J*17	Bronze	351 ~ 495	423	0.588
*J*18	Bronze	—	820	0.502
*P*1	Bronze	351 ~ 495	404	0.4
*P*2	Glass	—	393	0.4
*P*3	Copper	420 ~ 701	505	0.4
*P*4	Bronze	—	831	0.4
*P*5	Bronze	—	650	0.4
*P*6	Bronze	246 ~ 495	353	0.4
*P*7	Bronze	—	465	0.4

J—A sintered powder wick (J1, J2—a sintered non-spherical powder wick).
P—An unsintered powder wick.

Table 2. Working fluid properties at 20°C

Working fluid	ν ($m^2 s^{-1}$)	ρ ($kg m^{-3}$)	σ ($N m^{-1}$)
Pure water	1.010×10^{-6}	998.2	72.4×10^{-3}
Air*	15.63	116.6×10^{-2}	—
R-113	0.428	1567.0	23.7
SK. Oil No. 170	1.103	858.6	28.0
SK. Oil No. 240*	3.11	1017.2	—

* This working fluid used only for pressure drop test.

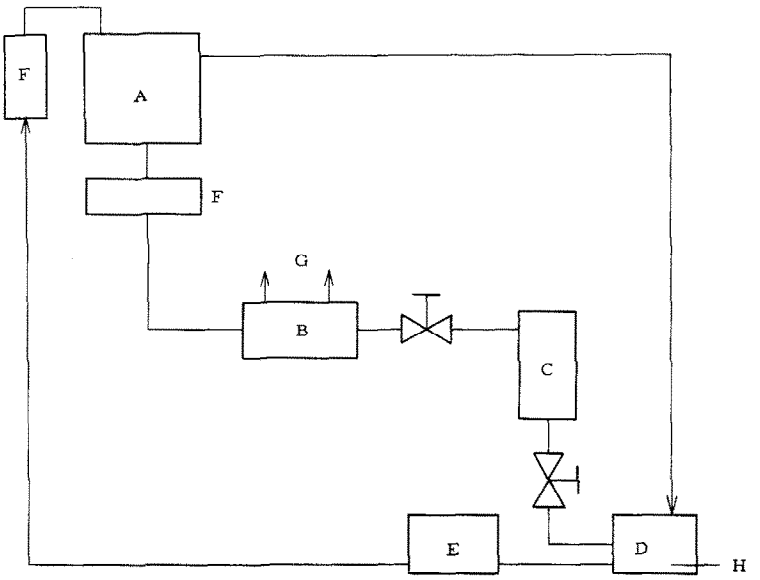

FIG. 1. Entire pressure drop apparatus system for steady-state method. A—Overflow tank; B—sample holder; C—flowmeter; D—stored tank; E—pump; F—filter; G—manometer; H—thermometer.

In an unsteady state method, flowrate Q was calculated from equation (3), and pressure drop ΔP_l from equation (4), which was obtained from equations (1), (2) and (3).

$$Q = A_t(H_I - H_F)/t \tag{3}$$

$$\Delta P_l = \rho_l \frac{H_I - H_F}{\ln\{(H_I - H_R)/(H_F - H_R)\}} g. \tag{4}$$

3.2. *Discussions of results*

The authors tried to correlate experimental results by the relation between friction factor f_K and Reynolds number N_{Re}. f_K and N_{Re} in a packed bed are often defined by the following equations, taking into consideration influences of particle diameter and porosity [8–10].

$$f_K = \frac{\Delta P_l D_p \varepsilon^3}{l \rho_l u_f^2 (1 - \varepsilon)} \tag{5}$$

$$N_{Re} = \frac{D_p u_f}{\nu_l (1 - \varepsilon)}. \tag{6}$$

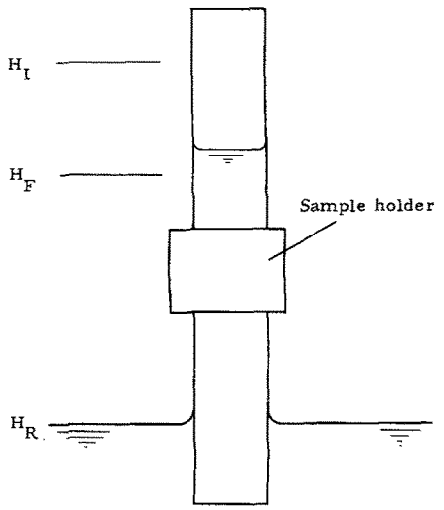

FIG. 2. Pressure drop apparatus for unsteady-state method.

Typical experimental results are shown in Fig. 3, presenting the relation between f_K and N_{Re}. Symbols J and P in the figure show a sintered powder wick and an unsintered powder wick (packed bed), respectively. The result is considered to be correlated by means of f_K and N_{Re}. From all the figures, the following experimental equation (7) is obtained. In the range of this experimental condition, difference between these two kinds of wick has not been clearly recognized.

$$f_K = 1.2 + \frac{180}{N_{Re}} \tag{7}$$

Reynolds number of liquid flow in the wick is normally small, and the first term of equation (7) is negligible, compared with the second term. So, equation (7) is rewritten by neglecting the first term and applying equation (2) to obtain.

$$K_p = \frac{1}{180} \frac{D_p^2 \varepsilon^3}{(1 - \varepsilon)^2}. \tag{8}$$

4. CAPILLARY FORCE

4.1. *Experimental outline*

Wick capillary force is obtained by measuring the height of liquid rising within the dry wick (the rising value—wick initially dry), or the height of a liquid column supported by the capillary force (the falling

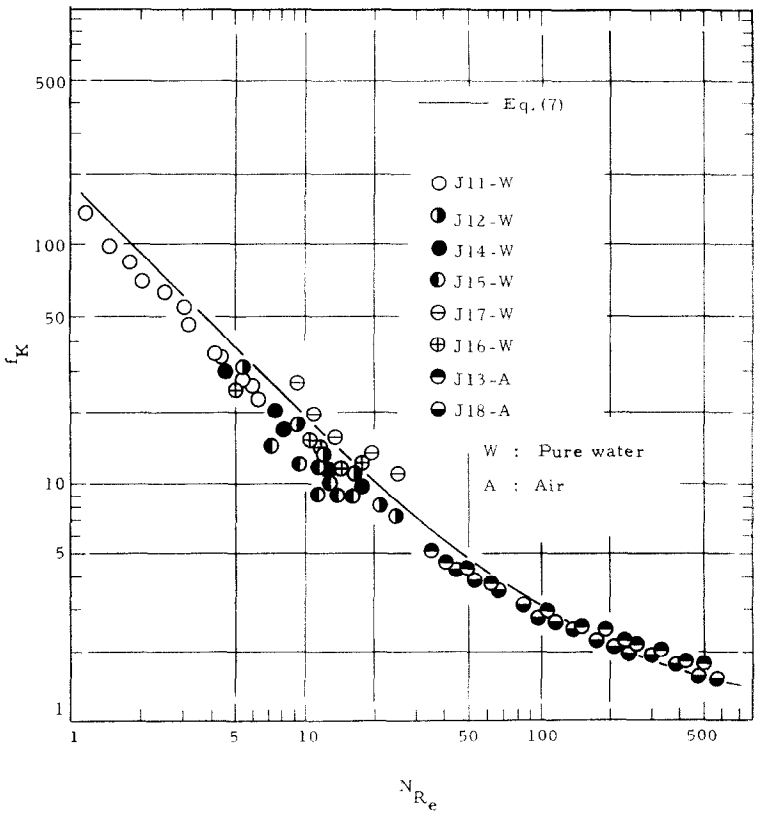

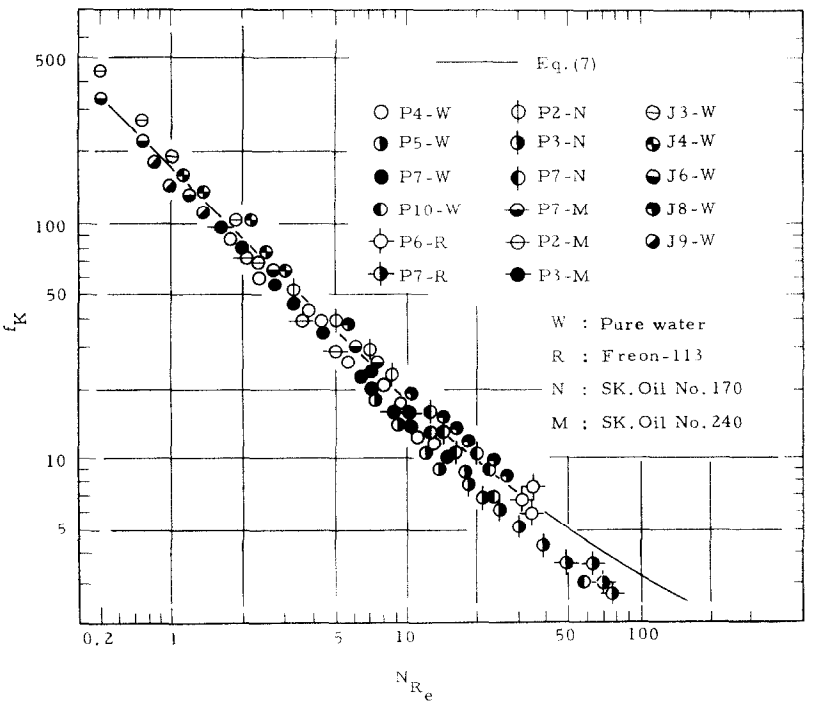

FIG. 3. Friction factor vs. Reynolds number.

value—wick initially saturated). However, it is known that there will be a difference between the two values, due to capillary hysteresis caused by variations in pore diameter. Normally, the rising value tends to be smaller than the falling value. A heat pipe operates with the wick initially saturated. All data used here will refer to the falling value, and will be referred to as the capillary equilibrium height. The maximum capillary pressure is obtained approximately from the following well-known relation.

$$\Delta P_C = \rho_l g h = \frac{4\sigma \cos\theta}{D_C}. \tag{9}$$

The apparatus used to determine the equilibrium capillary height is shown in Fig. 4 [2]. The sample is held horizontally in the sample holder shown on the left side of the figure. The glass tube on the right side can be moved in a vertical direction. At first, the liquid is filled up to the top of the sample to saturate it sufficiently and remove the air bubbles in it. The glass tube on the right side is lowered slowly, and the height from the lower end of the sample, as the liquid column supported by the sample drops, is the capillary equilibrium height.

Though qualitatively, it is reported that the surface condition of a wick is an important factor influencing the performance of a heat pipe [3]. This study included experiments to evaluate quantitatively the influence on the capillary force by the surface condition according to the cleaning procedures shown in Table 3.

4.2. *Discussion of results*

Kunz *et al.* [3] confirmed experimentally that the contact angle of Freon 113 on a solid surface was always 0 rad. For the same sample, the ratio of

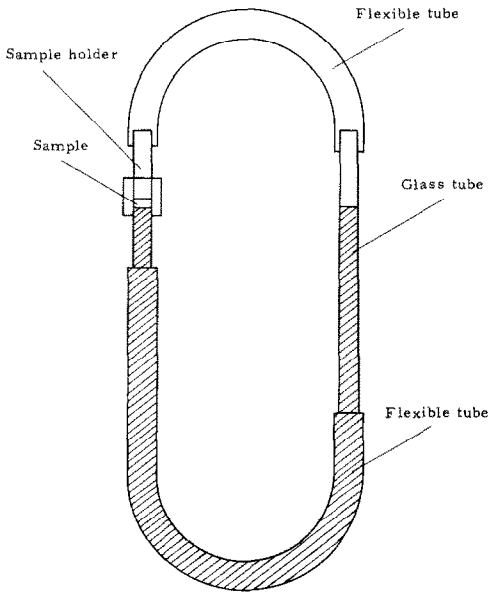

FIG. 4. Apparatus for determining capillary equilibrium height.

Table 3. Cleaning procedures

*CP*1	Wick is not cleaned
*CP*2	Wick is cleaned using a commercial detergent, it is then rinsed several times with pure water, then with acetone, and again with pure water
*CP*3	After *CP*2, wick is placed in an electric furnace and heated in air for 2 h (140, 200, 400, 650)*

* Values in parentheses are oxidation temperatures.

equilibrium heights of Freon 113 and distilled water is given by

$$\frac{(h)_W}{(h)_R} = \frac{\sigma_W}{\sigma_R}\,\frac{(\rho_l)_R}{(\rho_l)_W}\,\frac{(\cos\theta)_W}{(\cos\theta)_R}. \tag{10}$$

If both contact angles in equation (10) are 0 rad, then the ratio of equilibrium heights is 5.92 at 25°C. The ratios of values with equilibrium heights is listed in Table 4. As is clear from the table, the contact angle of water on the oxidized surface is considered to be almost 0 rad.

Then, using the concept of a hydraulic diameter for a packed bed, an attempt was made to induce the correlation to estimate the pore diameter of a sintered and an unsintered powder wick. Hydraulic diameter D_H may be expressed in the following way [11]:

$$D_H = 4 \times \left(\frac{\text{volume available for flow}}{\text{total wetted surface}}\right).$$

For a spherical powder,

$$D_H = \frac{2}{3}\,\frac{D_p \varepsilon}{(1-\varepsilon)}. \tag{11}$$

The comparison of D_H obtained from equation (11) with D_C from equation (9), based on the measured values of the equilibrium height, and the influence due to the surface condition, are shown in Fig. 5. The comparison of equation (11) with the measured values by [6] is shown in Fig. 6. As is clear from Fig. 5, the hydraulic diameter defined by equation (11) is considered to correspond approximately to the minimum pore diameter of the sintered and unsintered powder wicks. On the other hand, in the range of this experimental condition, the difference between the two kinds of wick has not been clearly recognized.

Table 4. Equilibrium capillary height and contact angle for pure water

Wick no.	$(h)_W$ (mm)	$(h)_R$ (mm)	$\frac{(h)_W}{(h)_R}$	Cleaning procedure
*J*8	418	70.0	5.98	*CP*3(200)*
*J*9	405	64.8	6.25	*CP*3(200)*
*J*10	251	44.0	5.70	*CP*3(200)*

* Values in parentheses are oxidation temperatures.

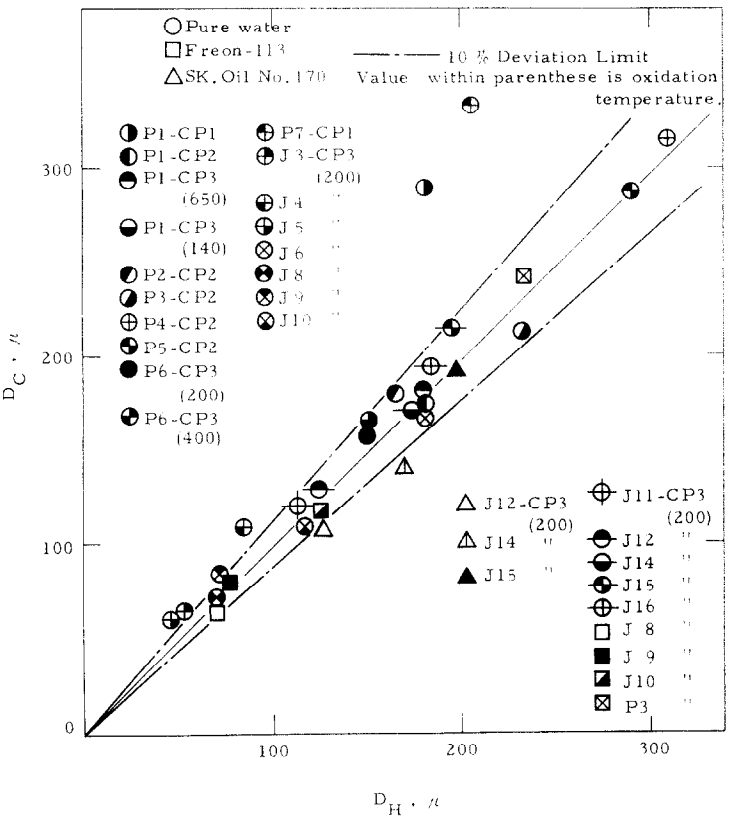

FIG. 5. Comparison of D_C and D_H.

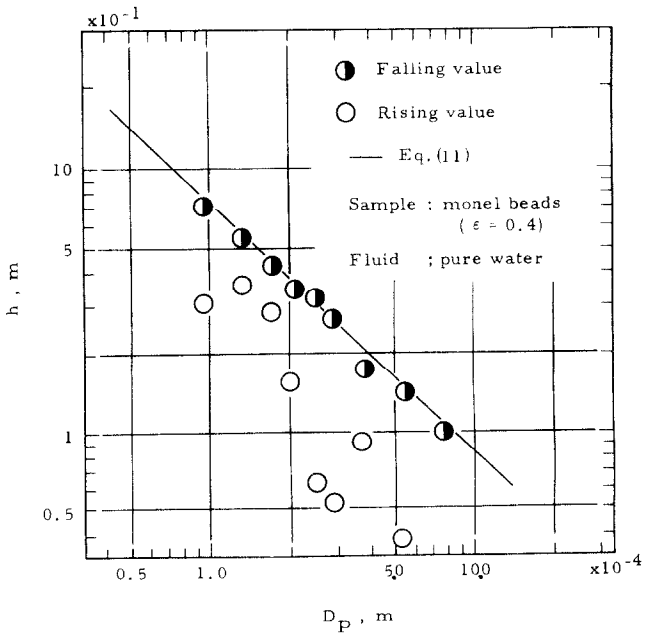

FIG. 6. Comparison of equation (11) and other results [6].

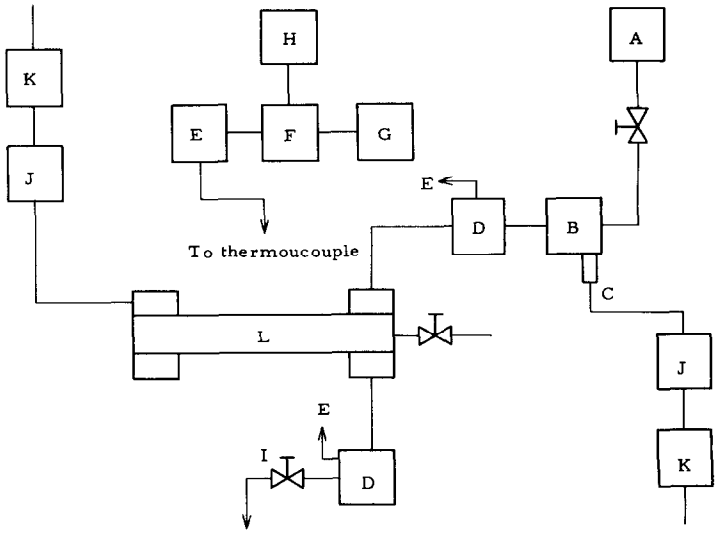

FIG. 7. Entire maximum heat-transfer rate experimental apparatus system: A—overflow tank; B—heating apparatus; C—pipe heater; D—mixing chamber; E—ice box; F—switch; G—self-registering thermometer; H—digital voltmeter; I—coolant water regulating valve; J—wattmeter; K—transformer; L—heat pipe.

5. MAXIMUM HEAT-TRANSFER EXPERIMENT

5.1. *Experiment outline*

The heat pipe container studied was a 304 stainless steel seamless tube with 28 mm I.D. and 32 mm O.D. Sintered powder metal, manufactured by sintering spherical metallic powder was used as a wick. With all heat pipes, cleanliness is of prime importance to ensure that no incompatibilities exist, and to make certain that the wick and wall will be wetted by a working fluid. As well as affecting the life of a heat pipe, negligence in assembly procedures can lead to an inferior performance, due, for example, to poor wetting. Accordingly, for assembling a heat pipe, care was taken in minimizing the contamination in a heat pipe, as well as the wick surface being oxidized (cleaning procedure CP3). Both ends of the heat pipe to be cleaned end in flanges, where the assembly is tested for leaks. When the heat pipe was vacuum tight, the requisite amount of pure water was fed into it. Ideally, the amount of liquid added should be just sufficient to saturate the wick. In practice, an additional amount has to be added to compensate for liquid accumulating in the fill tube. About 5 cc of excess water was added to these heat pipes. The fill tube was sealed with a vacuum valve. A drawing of the apparatus and descriptions of heat pipes are shown Fig. 7 and Table 5, respectively. A cylindrical heater block made of 5 cm long aluminum wound with electrical resistance wire, was used as the heat source and located at one end of the pipe. Heat was picked by the cooling water passing through a jacket fitted to the opposite end. Temperatures of pipe outer wall, at the inlet and outlet of cooling water, and of vapor were detected by 0.3 mm-dia. copper–constantan thermocouples, recorded by a self-registering thermometer and measured by a digital voltmeter, after confirming attainment of steady state.

Heat-transfer rate Q_e along the axis of the heat pipe was measured by employing the temperatures of water entering and leaving the jacket, and the flowrate by weighting. When the heat-transfer rate measured was compared with the electric input to the heater in the aluminum block, it was found that the heat loss is less than 5 per cent of the input. The temperature of the inner heated surface T_W at the evaporator was calculated from the following equation, assuming uniform heat flux.

Table 5. Heat pipe specification

	Pipe length (m)	Vapor space diameter (m)	Material	Particle size range (m)	Average particle size (m)	Porosity
*HP*1	483×10^{-3}	23.6×10^{-3}	Bronze	$246 \sim 495 \times 10^{-6}$	340×10^{-6}	0.420
*HP*2	480	22.4	Bronze	$495 \sim 701$	412	0.364
*HP*3	491	19.1	Bronze	$351 \sim 495$	433	0.323
*HP*4	490	23.6	Bronze	$250 \sim 420$	335	0.360
*HP*3	480	21.9	Copper	—	495	0.461

$$T_W = T_{W\text{out}} - \frac{\ln(D^*/D_{\text{in}})}{2\pi\lambda_s l_e}. \quad (12)$$

Average heat flux based on the area of the evaporator inner wall was calculated from the equation

$$q = \frac{Q_e}{\pi D_i l_e}. \quad (13)$$

5.2. *Measurement method of maximum heat-transfer rate*

The maximum heat-transfer rate was measured by the heat flux increasing method (HFI method) and the inclination angle increasing method (IAI method). In the HFI method, heat input was progressively increased, holding the inclination angle of the heat pipe and the vapor temperature constant, until the temperature measured at the upper extremity of the evaporator just began to rise rapidly. This heat-transfer rate was taken to be the maximum. On the other hand, IAI method made the heat pipe operate horizontally at any heat input, progressively increased the inclination angle, and regarded the inclination angle at the time of a rapid rise of evaporator wall temperature as the limit.

5.3. *Experimental results*

Figure 8(a) shows a typical plot of the temperature profile along the axis of the heat pipe. Temperature in the vapor space is constant for most of the experiments. Figure 8(b) shows an example of a rapid drop in vapor temperature in the condenser due to noncondensable gas.

Figure 9 shows heat flux-superheat result for HP5, together with change in the evaporator wall temperature at the limit. After measuring plot 2 data, heat flux was increased to 4.3×10^4 W m^{-2}. Then, the temperature at position c began to rise rapidly, as shown in Fig. 9(a), followed by a rapid temperature rise at position d. This phenomena is assumed to be due to expansion of the dryout area in the direction of the condenser. Judging from the wall temperature change at the limit, this limit is considered as the capillary wicking limit. The dot-chain line in the figure gives the result in the horizontal position under the same condition. Pipe inclination angle ϕ is considered to have no sensible effect on the heat transfer phenomena of the evaporator in the range of this experimental conditions. Figure 10 shows other results.

6. HEAT PIPE OPERATING LIMIT [12]

The wicking limit of a heat pipe is studied. In order for a heat pipe to operate, the pressure rise by capillary force must be greater than or equal to the sum of the pressure drops, as indicated in

$$\Delta P_c \geqq \Delta P_l + \Delta P_v + \Delta P_g. \quad (14)$$

The pressure difference due to the hydrostatic head of the liquid may either be positive, negative or zero, depending on the relative positions of the evaporator and condenser. This pressure difference ΔP_g is given by the expression

$$\Delta P_g = \rho_l g l_p \sin\phi \quad (15)$$

where ϕ is positive when the condenser is lower than the evaporator.

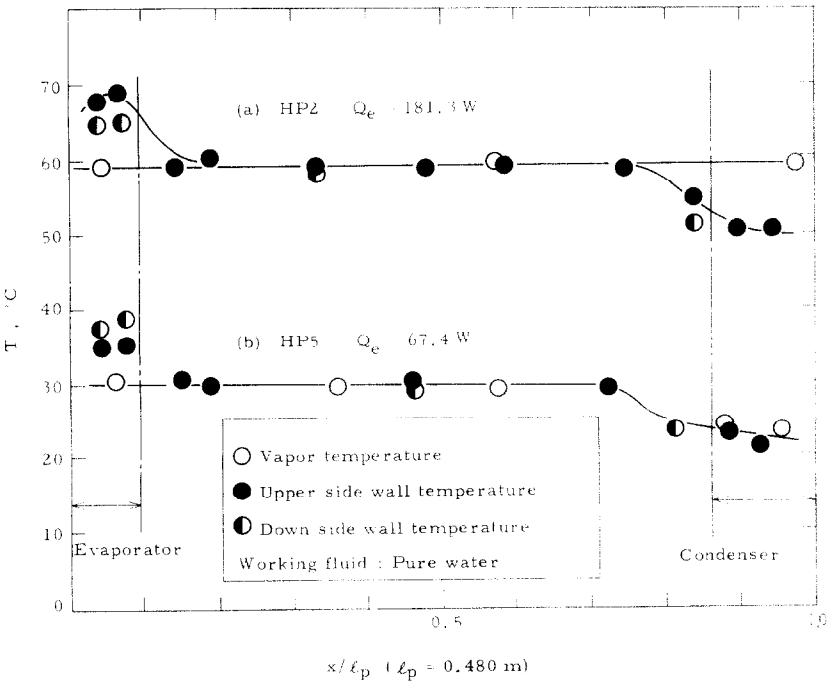

FIG. 8. Typical axial temperature distribution.

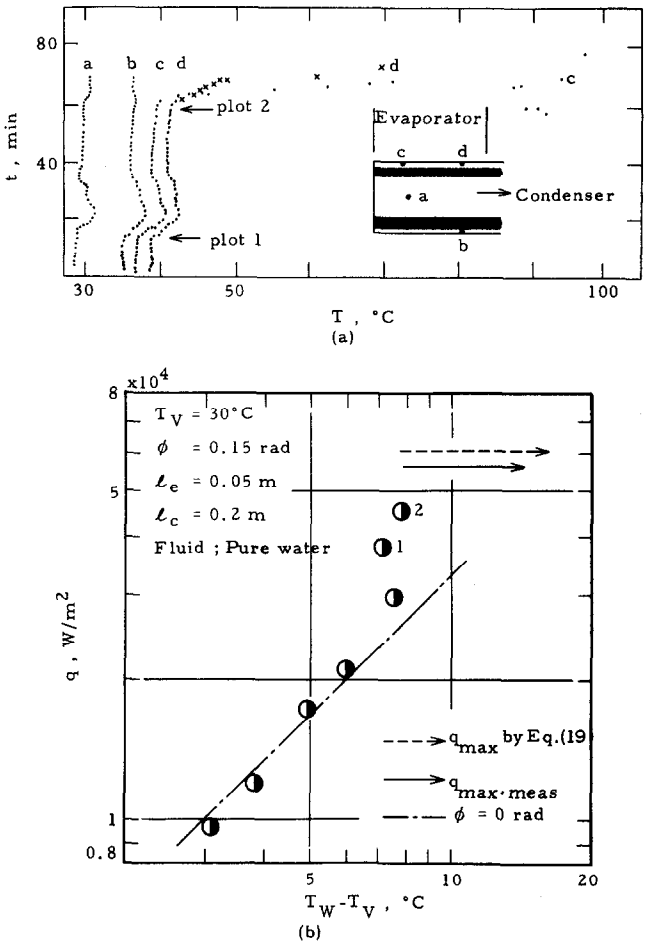

FIG. 9. Maximum heat-transfer data for *HP5* by HFI method.

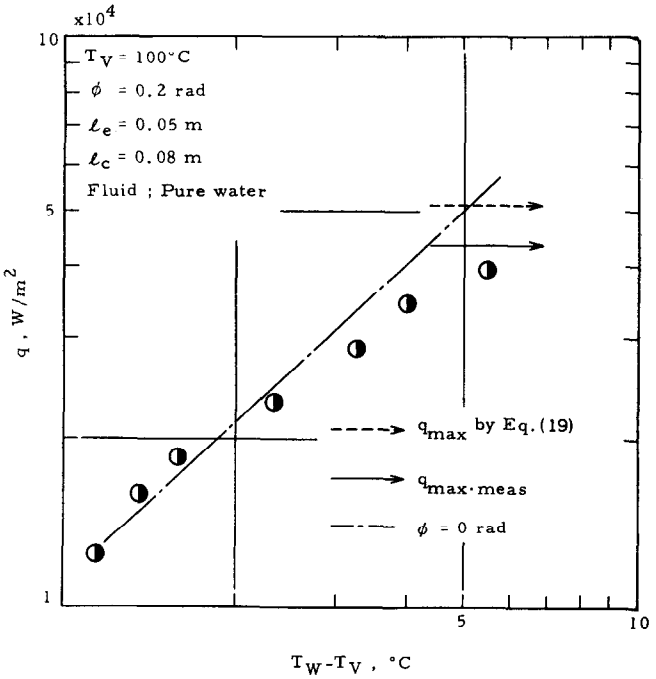

FIG. 10. Maximum heat-transfer data for *HP2* by HFI method.

The flow of liquid in a wick is described by Darcy's Law, as given by equation (2). For the case of one dimensional liquid flow in the heat pipe, equation (2) may be integrated to obtain the viscous liquid pressure drop in the wick ΔP_l, assuming the temperature along the heat pipe is uniform enough that v and ρ are essentially constant over the length of the heat pipe:

$$\Delta P_l = \frac{v_l}{k_p A_w}\left[\int_0^{l_c} m(x)_e \, dx + \int_{l_c}^{l_c+l_a} m(x)_a \, dx + \int_{l_c+l_a}^{l_p} m(x)_c dx\right]. \quad (16)$$

Linear mass injection in the evaporator and suction in the condenser are assumed. Thus, the mass flow rate in the evaporator is $m(x)_e = (m_l/l_e)\,x$, in the condenser is $m(x)_c = m_l(l_p - x)/l_c$ and in the adiabatic section is $m(x)_a = m_l$, where $m_l = Q_e/L$. Accordingly, equation (16) becomes

$$\Delta P_l = \frac{v_l Q_e}{k_p A_w L}\left(\frac{l_e}{2} + l_a + \frac{l_c}{2}\right). \quad (17)$$

The viscous vapor pressure drop ΔP_V had been analyzed by Cotter [1], but the analysis has some problems and does not always correspond with the experimental results [13]. In many heat pipe applications, however, $\Delta P_V \ll \Delta P_l$ as it is commonly treated [2, 3, 6, 12] and, since the vapor temperature along the heat pipe is almost constant in Fig. 8(a), no sensible error would practically be expected in calculating the capillary limited maximum heat transfer rate, even if ΔP_V was neglected.

The approximate wick maximum capillary pressure ΔP_C is obtained from equation (9).

For the limit of the heat pipe operation, equation (14) can be expressed as follows:

$$\Delta P_C = \Delta P_l + \Delta P_V + \Delta P_g. \quad (18)$$

By neglecting ΔP_V and substituting equations (9), (15) and (17) for ΔP_C, ΔP_g and ΔP_l, respectively into the above equation, the capillary limited maximum heat-transfer rate can be estimated by the equation

$$Q_{e\max} = L_m H_m V_m\left(1 - \frac{D_C \rho_l g l_p \sin\phi}{4\sigma\cos\theta}\right) \quad (19)$$

$$L_m = \frac{K_P}{D_C} \quad H_m = \frac{8A_W}{l_e + 2l_a + l_c} \quad V_m = \frac{L\sigma\cos\theta}{v_l}$$

7. COMPARISON

Comparisons of the maximum heat-transfer rates calculated from equation (19) using D_C from equation (11), K_P from equation (8) and fluid properties at the vapor temperature with measured values are shown in Figs. 9–11. With a heat flux of about 4.3×10^4 W m^{-2} ($Q_e = 170$ W) or less, equation (19) make it possible to predict the capillary limited maximum heat transfer rates with a tolerance of $\pm 20\%$. The measured values will be lower than the calculated values over about 4.3×10^4 W m^{-2}. The limit beyond this heat flux might be caused by change in the heat-transfer phenomena in the evaporator and not by the capillary wicking limit. The heat-transfer phenomena in the evaporator has not been fully studied yet. However, in high heat flux range, a state similar to a film boiling due to the high superheat, and the state of the vapor blocking of the pore in the wick might be aroused. A quantitative definition of the limit due to these phenomena necessitates further detailed studies on the heat-transfer

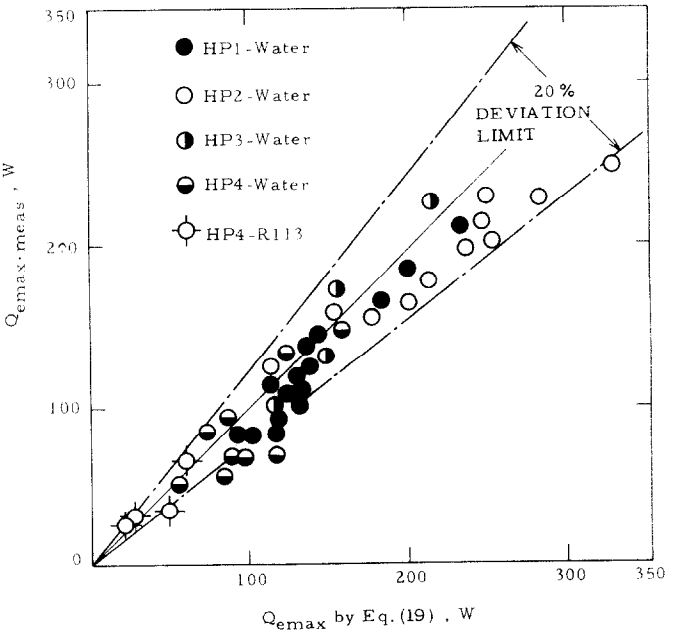

FIG. 11. Comparison of experimental and predicted maximum heat transfer rates by IAI method.

phenomena in the evaporator. However, the fact that the measured values go under equation (19) values in a high heat flux range, might be explained qualitatively by considering the decrease in the flow area in the wick due to local vapor blocking.

8. CONCLUSION

Preliminary experiments to recognize wick properties, and the maximum heat-transfer experiments were concluded. Results are:

(1) Pressure loss and capillary force of sintered and unsintered powder wick have been well correlated, as follows:

$$f_K = 1.2 + \frac{180}{N_{Re}}$$

$$0.3 < \varepsilon < 0.588$$

$$110 < D_P < 831\mu$$

$$0.5 < N_{Re} < 600$$

$$D_C = \frac{2}{3}\frac{\varepsilon D_P}{(1-\varepsilon)}$$

$$0.3 < \varepsilon < 0.54$$

$$110 < D_P < 831\mu.$$

(2) The degree of sintering that takes place between neighboring powders gives no sensible effect on the capillary force and the pressure loss.

(3) The liquid contact angle on the oxidized wick surface is 0 rad.

(4) The model proposed by this study makes it possible to predict the maximum heat-transfer rates for a limited capillary. The upper limit of heat flux applied to this model would vary according to the kind of working fluid, the kind and the dimensions of the wick etc., and in the range of this experimental condition, the upper limit of heat flux applied has been found to be approximately 4.3×10^4 W m^{-2}.

REFERENCES

1. T. P. Cotter, Theory of heat pipe, Los Alamos Sci. Lab., LA-3246-MS (1965).
2. E. C. Phillips, Low temperature heat pipe research program, NASA CR-66792 (1969).
3. H. R. Kunz *et al.*, Vapor chamber fin studies—transport properties and boiling characteristics of wicks, NASA CR-812 (1967).
4. J. K. Ferrell and H. R. Johnson, The mechanism of heat transfer in the evaporator zone of a heat pipe, ASME Paper No. 70-HT/SPT (1970).
5. J. H. Cosgrove, Engineering design of the heat pipe, Ph.D. Thesis, Dept. of Chemical Engineering, North Carolina State University (1966).
6. E. G. Alexander, Structure-property relationships in heat pipe wicking material, Ph.D. Thesis, Dept. of Chemical Engineering, North Carolina State University (1972).
7. A. E. Sheidegger, *The Physics of Flow Through Porous Media*, revised ed., p. 74. University of Toronto Press (1960).
8. I. Mogi, M. Tsutsumi, S. Kawai and T. Machiyama, Experimental investigations of the fundamental properties of sintered metal matrix applied to heat exchangers (in Japanese), *Bull. Sci. Engng Res. Lab. Waseda Univ.* **63**, 35–40 (1973).
9. E. Sabri, Fluid through packed columns, *Chem. Engng Prog. Symp. Ser.* **48**, 89–94 (1952).
10. F. E. Blake, Fluid flow through randomly packed columns and fluidized beds, *Trans. Am. Inst. Chem. Engrs.* **14**, 415–420 (1922).
11. R. B. Bird, W. E. Stewart and E. N. Lightfoot, *Transport Phenomena*, 1st ed., p. 197. John Wiley, New York (1959).
12. S. Shibayama, Heat pipe (in Japanese), *J. Japan Soc. Mech. Engrs* **74**, 861–865 (1971).
13. S. Nozu, T. Kamaya, A. Azuma, K. Shintani and E. Kozuka, Study on heat pipe (in Japanese), *Trans. Japan Soc. Mech. Engrs* **35**, 392–401 (1969).

ETUDE SUR LES TUBES A CHALEUR

Résumé—le but de cette étude était d'obtenir une connaissance sur les limites du fonctionnement des tubes à chaleur.

Les poudres frittées ont été utilisées comme mèche, l'eau pure et le Fréon 113 comme fluide circulant. Dans cette étude deux séries d'expériences ont été entreprises. La première comportaint des études, indépendantes les unes des autres, de la déperdition par le frottement, des propriétés capillaires et des caractéristiques de la mèche. La seconde consistait à mesurer le rendement maximal du transfert de chaleur. Le modèle simplifié a été développé pour le calculer aux limites capillaires. Sa valeur expérimentale était parfaitement conforme à sa valeur théorique calculée sur le modèle.

STUDIUM ÜBER HEIZUNGSRÖHRE

Zusammenfassung—Das Ziel des Studium iet das Verständnis von der Heizungsröhre, die die Grenzen handhabt, zu bekommen.

Gesinternes Pulver wird als Docht benutzt, und reines Wasser und Freon 113 als Arbeitsflüssigkeit. In dem Studium wurden zwei Typen vom Experiment unternommen. Der erste enthielt unabhängige Studien über Dochtseigenschaft, Reibungsverlust und Kapillarität. Der zweite enthielt die Messung vom Höchstwärmeübergangswert. Das vereinfachte Model wurde entwickelt, um den Höchstwärmeüberganswert der Kapillargrenzen vorauszusagen. Die Übereinstimmung zwischen den vorausgesagten und experimentellen Höchstwärmeübergangswerten war ausgezeichnet.

ИССЛЕДОВАНИЕ ТЕПЛОПРОВОДНОЙ ТРУБЫ

Аннотация — Данное исследование проведено с целью узнать эксплуатационные пределы для этой трубы.

В качестве фитиля применяли агломерационные порошки, а в качестве рабочей жидкости были пользованы чистая вода и Фреон 113. Для этого исследования были проведены 2 типа испытания. В одном типе испытания изучали характеристики фителя, потери на трение и капиллярное свойство.

В другом испытании был определен коэффициент теплопередачи. Для прогнозирования максимального коэффициента теплопередачи предельной капиллярности были разработаны упрощенные модели. Результаты испытания максимального коэффициента теплопередачи прекрасно согласуются с прогнозированными величинами.